Anions of Tridentate SPS Ligands: Syntheses, X-ray Structures and DFT Calculations

Marjolaine Doux,[†] Pierre Thuéry,[‡] Matthias Blug,[†] Louis Ricard,[†] Pascal Le Floch,[†] Thérèse Arliguie,*[,‡] and Nicolas Mézailles*[,†]

Laboratoire ''Hétéroéléments et Coordination'', Ecole Polytechnique, CNRS, 91128 Palaiseau Cédex, France and Service de Chimie Moléculaire, DSM, DRECAM, CNRS URA 331, CEA/Saclay, 91191 Gif-sur-Yvette cedex, France

Received July 2, 2007

Reaction of 2,6-bis(diphenylphosphine sulfide)-3,5-diphenylphosphinine (SPS) (**1**) with alkyllithium reagents (MeLi, *n*-BuLi, Li−methyl pyridine) led to formation of the stable lithium salts $[Li(THF)_2][SPS^{(Me)}]$ (**2**), $[Li(THF)_2][SPS^{(n-Bu)}]$ (**3**), and $[Li(THF)_2][SPS^{(CH2Py)}]$ (**12**) by a nucleophilic attack on the central phosphorus atom of the phosphinine ring, whereas treatment of **1** with *t*-BuLi led to the intermediate formation of $[Li(THF)_2][SPS^{(t-Bu)}]$ (**4**) followed by elimination of isobutene and formation of $[Li(THF)_2][SPS^{(H)}]$ (**5**). By addition of optically pure lithium (−)-mentholate or (−)-menthyl Grignard reagent to **1** the chiral derivatives $[Li(THF)_2][SPS^{(OMen)}]$ (**6**) and $[Li(THF)_2][SPS^{(Men)}]$ (**9**) were obtained, respectively. The potassium salt of the anionic SPS pincer ligand $[K(THF)_2][SPS^{(Me)}]$ (**10**) was isolated from a salt exchange reaction of **2** with *t*-BuOK in diethyl ether. Coordination of BH_3 to the central phosphorus atom in compound $[K([18]crown-6)THF)][SPS^{(Me)}\cdot BH_3]$ (**11**) confirmed the phosphine character of the hypervalent λ^4 phosphorus atom. The X-ray crystal structures of compounds **2a**, **2b**, **10**, and **12** reveal the flexibility of the $[SPS^{(Me)}]$ anion ligand. Finally, the difference in the electronic properties and structural features of compounds **2a** and **2b** were investigated by means of DFT calculations and a NBO analysis.

Introduction

The coordination chemistry of pincer ligands has been a rapidly growing field of investigations over the past decade. Among the various combinations the "PCP−metal" fragments have found applications in fundamental processes such as C−H activation as well as in several catalytic processes.[1] Over the past few years we have been interested in the use of $SPS^{(R)}$ tridentate anionic ligands synthesized from a common precursor, 2,6-bis(diphenylphosphine sulfide)-3,5-diphenylphosphinine (SPS), bearing a central phosphinine ring with two diphenylphosphinosulfide pendant arms. These $SPS^{(R)}$ ligands have shown an ability to coordinate not only electron-rich metal centers, such as Cu(I) and Au(I),[2] but also very electron-poor metal fragments, such as early Ln(III) or U(IV).[3] In the course of our studies cross-coupling catalysis with Pd(II) was developed[4,5] as well as activation of CS_2, O_2, and SO_2 with Rh(I).[6] Most importantly, this ligand also proved highly flexible, allowing any potential geometry at a metal center to be stabilized (square planar, tetrahedral, octahedral, etc.).[7] Indeed, variations of the oxidation state at the metal center often encountered in catalytic cycles may be accompanied by significant changes in geometries which have to be accessible to the ligand structure. In all cases, coordination of the $SPS^{(R)}$ anion occurred in a tris η^1 (P,S,S) fashion. It is in contrast with what was previously observed for mono "phosphinine−anion" ligands for which in the rare cases of η^1 coordination (type C complex) the resulting complexes proved to be very unstable (Scheme 1).

In 2003, a structural study of several monophosphinine anionic derivatives, combined with DFT calculations, allowed us to rationalize the electronic structure of these species as being a cyclohexadienyl anionic fragment and a phosphine fragment.[8] In the case of the $SPS^{(R)}$ anion, two resonance structures have been proposed in order to rationalize the geometric features found in several complexes (Scheme 2).[9] In form A the charge is delocalized from one sulfur atom to the other and the central phosphorus is a classical phosphine. On the other hand, in form B the charge is mainly localized on the phosphorus atom and the structure would derive from a 1-*H*-λ^5-phosphinine (hypervalent phosphorus center).

Our purpose here is four-fold. First, the tris η^1 (P,S,S) coordination is rationalized in terms of a simple orbital perturbation diagram. Second, we wish to present the extension of the synthetic method to production of unknown chiral $SPS^{(R)}$

* To whom correspondence should be addressed. N.M.: phone, +33 1 69 33 44 14; fax, +33 1 69 33 44 49; e-mail, nicolas.mezailles@polytechnique.edu. T.A.: phone, +33 1 69 08 60 42; fax, +33 1 69 08 66 40; e-mail, therese.arliguie@cea.fr.

[†] Ecole Polytechnique.

[‡] Service de Chimie Moléculaire, DSM, DRECAM.

(1) Albrecht, M.; Van Koten, G. *Angew. Chem., Int. Ed.* **2001**, *40*, 3750.

(2) Doux, M.; Ricard, L.; Le Floch, P.; Mezailles, N. *Dalton Trans.* **2004**, 2593.

(3) Arliguie, T.; Doux, M.; Mézailles, N.; Thuery, P.; Le Floch, P.; Ephritikhine, M. *Inorg. Chem.* **2006**, *45*, 9907.

(4) Doux, M.; Mézailles, N.; Melaimi, M.; Ricard, L.; Le Floch, P. *Chem. Commun.* **2002**, 1566.

(5) Doux, M.; Bouet, C.; Mézailles, N.; Ricard, L.; Le Floch, P. *Organometallics* **2002**, *21*, 2785.

(6) Doux, M.; Mézailles, N.; Ricard, L.; Le Floch, P. *Organometallics* **2003**, *22*, 4624.

(7) Doux, M.; Mézailles, N.; Ricard, L.; Le Floch, P.; Vaz, P. D.; Calhorda, M. J.; Mahabiersing, T.; Hartl, F. *Inorg. Chem.* **2005**, *44*, 9213.

(8) Moores, A.; Ricard, L.; Le Floch, P.; Mézailles, N. *Organometallics* **2003**, *22*, 1960.

(9) Doux, M.; Piechaczyk, O.; Cantat, T.; Mézailles, N.; Le Floch, P. *C. R. Chimie* **2007**, *10*, 1.

10.1021/om7006634 CCC: $37.00
Publication on Web 10/09/2007

Scheme 1

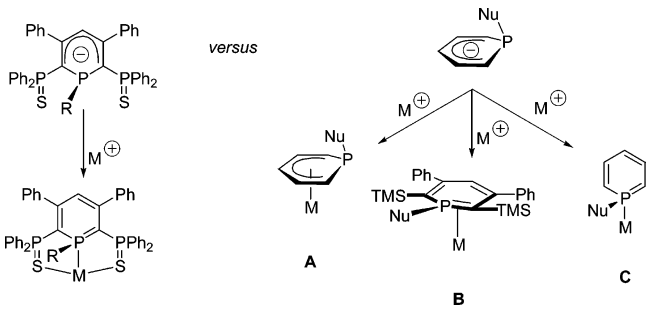

Scheme 2

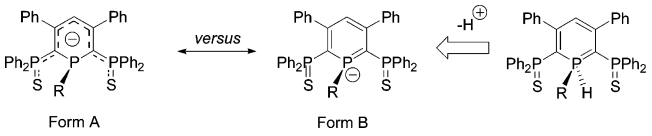

Scheme 3

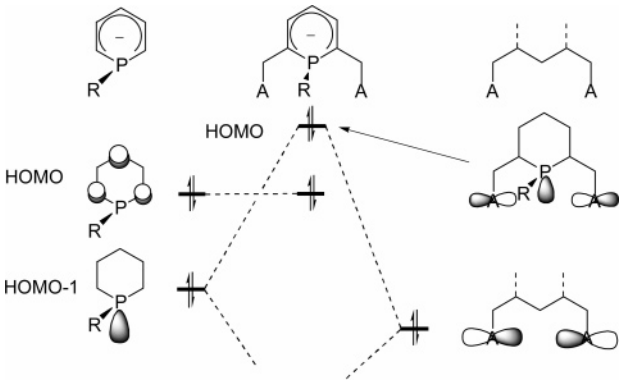

anionic derivatives and a tetradentate ligand. Third, a precise structural analysis was allowed by crystallization of several anionic derivatives. Finally, DFT calculations and NBO (natural bond orbital) analysis performed on these systems will be presented. These full analyses will allow us to give a precise description for the $SPS^{(R)}$ anion.

Results and Discussion

How To Favor Tris η^1 (P,S,S) Coordination Mode. As mentioned above, early literature reports showed the η^5 coordination of anions of phosphinines to be favored over the η^1 coordination. In line with these results, DFT calculations showed that the HOMO-1 possesses a large coefficient at the phosphorus center and therefore mostly describes the lone pair of the anion. On the other hand, the HOMO of the system is mainly localized on the carbon atoms at the 2, 4, and 6 positions, consistent with the cyclohexadienyl representation (left-hand side, Scheme 3). With this simplified diagram in mind we reasoned that adding two ancillary ligands bearing lone pairs with appropriate symmetry (and of lower energy) would result in a destabilizing four-electron interaction which would raise in energy the orbital of the lone pair at phosphorus.

It was then verified by DFT calculations[10,11] (B3LYP[12−14]/6-31+G*[15]) using the Gaussian03 set of programs[16] on two model compounds that the two orbitals HOMO-1 and HOMO are indeed swapped in the two systems (Figure 1).

In accordance with the simplified orbital diagram, the HOMO of the SPS system is mostly developed on the phosphorus center and on the two sulfur centers to a lesser extent. It is thus best described as three lone pairs: one at the phosphorus center and two at the sulfur atoms. The interaction is clearly an anti phase

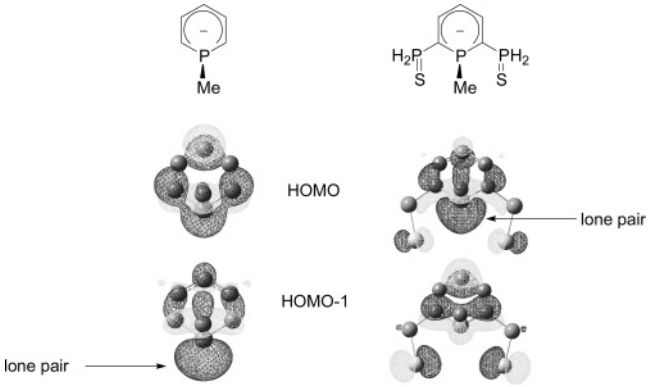

Figure 1. HOMO and HOMO-1 orbitals of the 1-methyl-λ^4-phosphinine anion and of the 1-methyl anion of the SPS phosphinine.

interaction between the sulfur lone pairs and the phosphorus lone pair as predicted by the simple perturbation diagram. Because of the nonplanarity of the system, coefficients are also found on the carbon centers of the ring.

Synthesis of $SPS^{(R)}$ Anions. As shown previously, the phosphorus center of a phosphinine ring is electrophilic.[8,17−23] In general, however, the phosphinines are stable toward addition of neutral nucleophiles, such as water or alcohols, even in solution. On the other hand, SPS ligand **1** was shown to react readily with the same nucleophiles to lead to the corresponding 1,1-disubstituted λ^5 derivatives, which were subsequently reacted with group 10 metal centers.[24] This is rationalized by the presence of two electron-attracting substituents at the 2 and 6 positions which increase the electrophilicity of the phosphorus center. A straightforward approach was subsequently developed by reacting **1** with charged nucleophiles such as MeLi or *n*-BuLi leading to anions **2** and **3**, respectively (eq 1).[4] These highly reactive anions were then reacted, without further purification, with the desired metal precursors.[6,24] Upon addition of the nucleophile, the central phosphorus experiences a very high upfield shift from +250 to about −60 ppm in the ^{31}P NMR spectrum.[2] This tremendous variation of about − 310 ppm of the central phosphorus atom chemical shift from **1** to **2** or **3** is by itself proof of the change of sp^2 hybridization to sp^3 hybridization. In fact, it also shows the aromaticity of the ring to be disrupted, and the chemical shift is very close to that of the very basic phosphine, PMe_3 (−63 ppm). On the other hand, the chemical shift of the PPh_2S moiety is not altered to a great extent: $\Delta\delta = 2.5$ ppm (**1**, $\delta = 43.4$ ppm).

(10) Ziegler, T. *Chem. Rev.* **1991**, *91*, 651.
(11) Parr, R. G.; Yang, W. *Density Functional Theory of Atoms and Molecules*; Oxford University Press: Oxford, Royaume Uni, 1989.
(12) Becke, A. D. *Phys. Rev. A* **1988**, *38*, 3098.
(13) Lee, C.; Yang, W.; Parr, R. G. *Phys. Rev. A* **1988**, *B 37*, 785.
(14) Perdew, J. P. *Phys. Rev. B* **1986**, *33*, 8822.
(15) Clark, T.; Chandrasekhar, J.; Spitznagel, G. W.; von Ragué Schleyer, P. *J. Comput. Chem.* **1983**, *4*, 294.
(16) Frisch, M. J. et al. *Gaussian 03 W* (Revision C.02); Gaussian, Inc.: Wallingford, CT, 2004.
(17) Märkl, G.; Heier, K.-H. *Angew. Chem., Int. Ed.* **1972**, *11*, 1016.
(18) Märkl, G.; Lieb, E.; Merz, A. *Angew. Chem., Int. Ed.* **1967**, *6*, 86.
(19) Märkl, G.; Merz, A. *Tetrahedron Lett.* **1968**, *32*, 3611.
(20) Märkl, G.; Merz, A. *Tetrahedron Lett.* **1969**, *10*, 1231.
(21) Märkl, G.; Merz, A. *Tetrahedron Lett.* **1971**, *17*, 1215.
(22) Ashe, A. J., III; Smith, T. W. *J. Am. Chem. Soc.* **1976**, *98*, 7861.
(23) Ashe, A. J., III; Smith, T. W. *Tetrahedron Lett.* **1977**, *5*, 407.
(24) Doux, M.; Mézailles, N.; Ricard, L.; Le Floch, P. *Eur. J. Inorg. Chem.* **2003**, 3878.

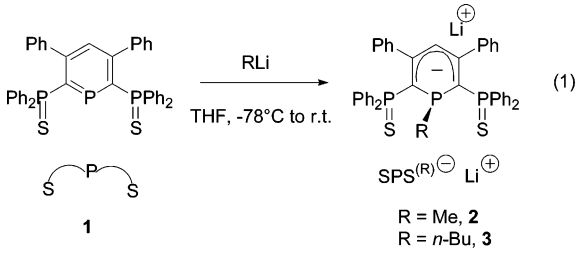

(1)

In **2** the ^{1}H NMR signal of H4 is found 1.8 ppm upfield from the one observed for **1**. In the ^{13}C NMR spectrum C2 and C6 are not only found at very high field (73.6 ppm, $\Delta\delta = -86.1$ ppm) but the magnitude of the coupling constant J(C−P) decreased dramatically (^1J(C2−P) = 6.0 in **2** vs 66.2 Hz in **1**). The C4 atom is also high-field shifted ($\Delta\delta = -20.3$ ppm), whereas the C3 and C5 atoms are barely modified ($\Delta\delta = +5.5$ ppm). These NMR data are consistent with what was found previously by Ashe on the anion of the parent phosphinine C_5H_5P and by us on other phosphinine derivatives. Therefore, on the basis of the NMR data, the description "Form A" would be favored.

It is well known that substituent effects, steric or electronic, may have a tremendous impact on a catalytic process. Use of a common precursor, ligand **1**, was thus envisioned as an entry into several other anions with varied substitution schemes. In a first attempt, because of the performance of the highly donating sterically demanding P(*t*-Bu)$_3$ ligand in several Pd-catalyzed cross-coupling processes, reaction of **1** with *t*-BuLi in THF at low temperature was carried out. The desired anion **4** was obtained quantitatively as verified by ^{31}P NMR spectroscopy (eq 2). It is characterized by a triplet at −43.1 ppm (^2J(P−P) = 158.0 Hz, *t*-BuP) and a doublet at 46.2 ppm (PPh_2S). Compared to anion **2**, the central phosphorus atom in **4** is downfield shifted by 22.6 ppm, which is consistent with the difference in chemical shifts for P(Me)$_3$ and P(Me)$_2$(*t*-Bu).[25] This anion appeared however quite unstable, leading to a new species within 30 min at room temperature, also characterized by a triplet at high field (**5**, $\delta = -73.7$ ppm). Most interestingly, the ^{1}H-coupled ^{31}P NMR spectrum proved the presence of a new P−H bond as evidenced by a large coupling constant ^1J(P−H) = 195.8 Hz. It appeared that elimination of 2-methylpropene from **4** had occurred. This was subsequently verified on a small-scale reaction in THF-d_8 in a sealed NMR tube. Indeed, due to partial solubility of 2-methylpropene in the solvent at room temperature, the expected signals were observed by ^{1}H NMR spectroscopy. This type of elimination is not observed when groups other than PPh_2S are bound to the phosphinine ring, and DFT calculations are being carried out in order to elucidate the precise mechanism.

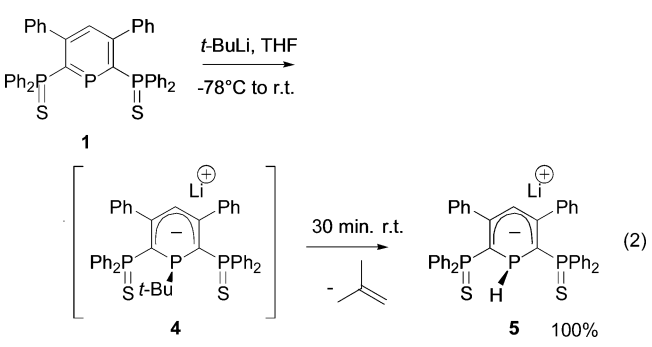

(2)

1 was also used as a precursor to optically pure anions via simple transformations. Indeed, reaction with lithium (−)-mentholate resulted in formation of ligand **6** in quantitative yield (eq 3).

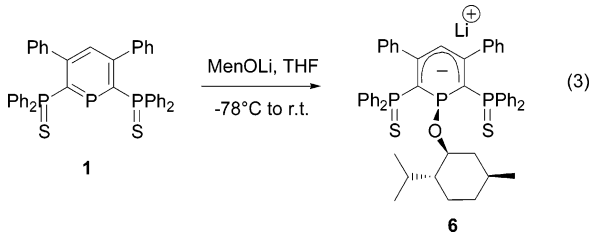

(3)

As expected, the presence of a chiral substituent at the phosphorus center induces a magnetic inequivalence of the two ancillary PPh_2S moieties ($\delta = 45.1$ and 45.4 ppm). The central phosphorus atom appears as a pseudo triplet at 61.8 ppm (^2J(P−P) = 176.2 Hz), a chemical shift typical for phosphinites. Synthesis of anion **7**, possessing (−)-menthyl as the phosphorus substituent, was more complicated as it is known that the menthyllithium epimerizes in solution.[26] The Grignard analogue which is configurationally stable was thus used.[27,28] Reaction of this species with **1** was however sluggish, and an excess of Grignard was required to drive the reaction to completion (Scheme 5).

The reaction mixture was hydrolyzed to lead first to a λ^5-phosphinine, **8a**, which isomerized partially into two dihydrophosphinines, **8b** and **8c**, within 30 min. Compound **8a** disappeared totally within 2 h, concomitant with formation of a mixture of **8b** and **8c** in an approximate ratio of 1/0.2. The final equilibrium was reached after several days: **8b**/**8c** of 2/1. Compound **8a** was characterized in ^{31}P and ^{1}H NMR spectroscopies by a large ^1J(H−P) (493.9 Hz) coupling constant, typical of a P^V−H bond. Thus, in a typical procedure complete formation of **8a** was checked by ^{31}P NMR and the reaction mixture was taken to dryness in order to prevent the isomerization process from occurring. The compound is purified by column chromatography, and pure **8a** was quantitatively deprotonated with MeLi to yield the desired lithium derivative **9**. Note that the deprotonation process can also be performed equally well with a mixture of isomers **8a**−**c**. As in the case of **6**, the chiral substituent induces a magnetic inequivalence of the two PPh_2S moieties. The central phosphorus center resonates therefore as a doublet of doublets at −45.1 ppm (^2J(P−P) = 153.1 Hz and ^2J(P−P) = 159.2 Hz). This chemical shift is quite similar to the one of **4**, also bearing a bulky substituent.

We reported very recently the use of $SPS^{(Me)}$ anions in the stabilization of several U(IV) centers and lanthanides. In the course of these studies it was necessary to change the Li counterion to K. Indeed, upon reaction of a $SPS^{(R)}$ anion with U−X (X = Cl, BH_4) precursors a salt is formed which may react with the complex formed to yield an "ate complex". Not common with transition-metal complexes, this "ate complex" formation becomes very favorable with f metals and may be formed with all cations, Li, Na, or K. One way to circumvent this problem is to form a byproduct that is insoluble in the reaction medium, which is the case for KCl and KBH_4 in

(25) Mann, B. E. *J. Chem. Soc., Perkin Trans. 2* **1972**, 30.
(26) Maercker, A.; Schuhmacher, R.; Buchmeier, W.; Lutz, H. D. *Chem. Ber.* **1991**, *124*, 2489.
(27) Smith, J. G.; Wright, G. F. *J. Org. Chem.* **1952**, *17*, 1116.
(28) Beckmann, J.; Dakternieks, D.; Drager, M.; Duthie, A. *Angew. Chem., Int. Ed.* **2006**, *45*, 6509.

Scheme 4

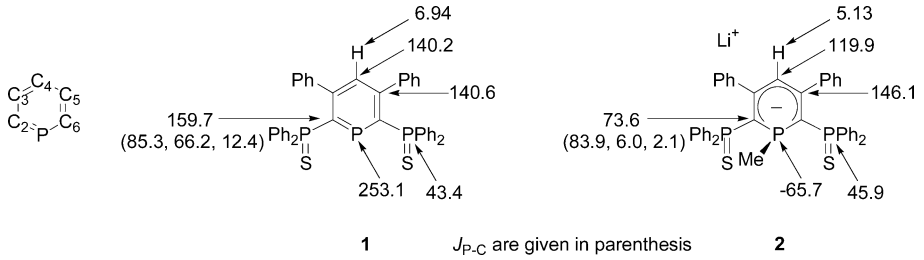

Scheme 5

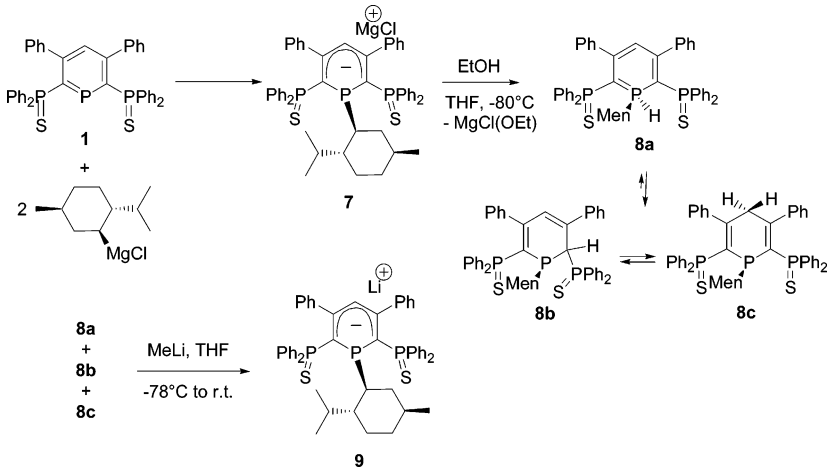

THF.[29,30] The potassium analogue of **2**, **10**, was therefore synthesized via a Li/K exchange in the presence of *t*-BuOK in diethyl ether at low temperature (eq 4).[31−35]

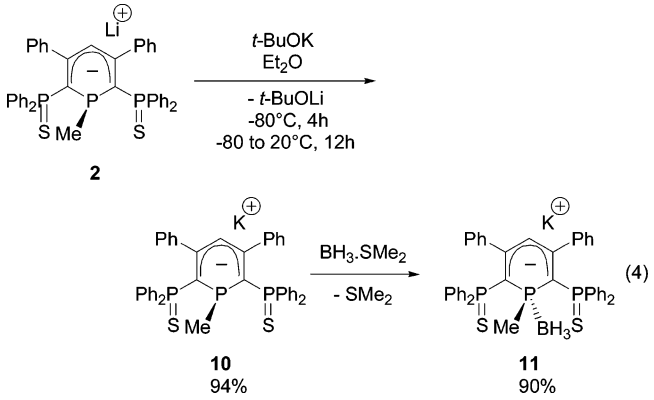

Anion **10** was fully characterized by usual NMR techniques. In fact, only minor differences are found between the spectra of **2** and **10**. However, these differences clearly point to formation of a new species and coordination to a different metal center. For example, in the same solvent the two phosphorus signals are shifted by −2.8 (PPh_2S) and +3.7 ppm (PMe). More evidence for cation exchange was provided by an X-ray diffraction study. Crystals were obtained by slow diffusion of hexanes into a THF solution of **10**. An ORTEP plot is presented in Figure 2. Surprisingly, the structure is dimeric, one potassium atom is bound to a SPS fragment via the P atom and one S atom and to another SPS unit via one sulfur atom. Tris η^1 coordination is also favored. The bond lengths and angles found in **10** are typical of these anions and will be discussed further below in the case of **2**. One may note however the pyramidality of the phosphorus center (Σ angles = 302.3°), typical of a sp^3-hybridized center, and the similarities in the C−C bond distances of the ring (1.394(2)−1.410(2) Å) indicating delocalization of the charge over the five carbon atoms.

In order to confirm the "phosphine" character of the central phosphorus atom, its coordination to a borane was carried out. The resulting anion **11** was characterized by ^{1}H, ^{11}B, and ^{31}P NMR. The chemical shifts in both the ^{11}B NMR spectrum (broad singlet at −37.3 ppm, $w_{1/2}$ = 290.0 Hz) and in the ^{31}P NMR

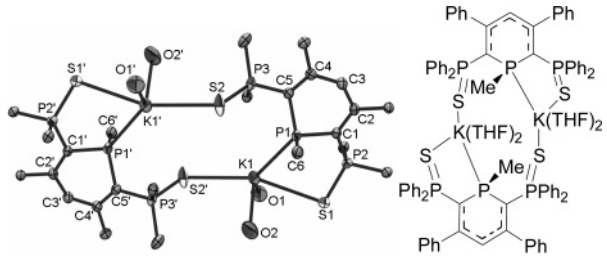

Figure 2. Structure (50% probability ellipsoids) of **10**. Phenyl groups were omitted for clarity. Bond distances (Å) and angles (deg): P1−C1 1.824(1), C1−C2 1.394(2), C2−C3 1.410(2), C3−C4 1.402(1), C4−C5 1.398(2), C5−P1 1.811(1), C6−P1 1.844-(1), C1−P2 1.778(1), C5−P3 1.761(1), P2−S1 1.9768(4), P3−S2 1.9775(5), P1−K1 3.2712(5), S1−K1 3.3793(4), S2′−K1 3.2962-(5), O1−K1 2.711(1), O2−K1 2.800(2), C1−P1−C5 99.49(5), P1−C1−C2 118.33(8), C1−C2−C3 122.9(1), C2−C3−C4 125.6(1), C3−C4−C5 121.6(1), C4−C5−P1 118.28(7), (mean plane C1−C2−C4−C5)−P1 22.2, (mean plane C1−C2−C4−C5)−C3 5.5.

(29) Schumann, H.; Meese-Marktscheffel, J. A.; Esser, L. *Chem. Rev.* **1995**, *95*, 865.
(30) Evans, W. J.; Peterson, T. T.; Rausch, M. D.; Hunter, W. E.; Zhang, H.; Atwoodld, J. L. *Organometallics* **1985**, *4*, 554.
(31) Schlösser, M.; Strunck, S. *Tetrahedron Lett.* **1984**, *25*, 741.
(32) Schlösser, M. *Pure Appl. Chem.* **1988**, *60*, 1627.
(33) Fernández-Galán, R.; Hitchcock, P. B.; Lappert, M. F.; Antiñolo, A.; Rodríguez, A. M. *J. Chem. Soc., Dalton Trans.* **2000**, 1743.
(34) Woodman, T. J.; Schormann, M.; Bochmann, M. *Organometallics* **2003**, *22*, 2938.
(35) Woodman, T. J.; Schormann, M.; Hughes, D. L.; Bochmann, M. *Organometallics* **2003**, *22*, 3028.

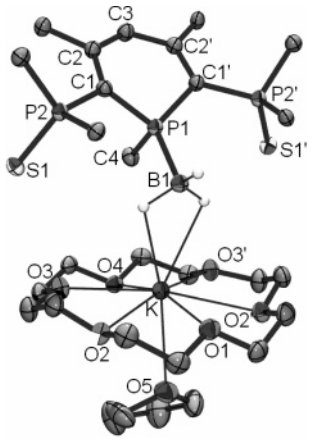

Figure 3. ORTEP plot (50% probability ellipsoids) of **11**. Phenyl groups are omitted (distances (Å) and angles (deg)): P1−C1 1.801(3), C1−C2 1.404(4), C2−C3 1.406(3), C3−C2′ 1.406(3), C2′−C1′, P1−C1′ 1.801(3), P1−C4 1.822(4), P2−C1 1.782(3), S1−P2 1.973(1), P1−B1 1.945(5), P1−K 3.343(5), B1−H···K 1.140, B1−H 1.089, H−K 2.822, C1−P1−C1′ 102.0(2), Σ angles P1 = 309.7.

spectrum (broad singlet at 2.9 ppm, $w_{1/2}$ = 165.0 Hz) are analogous to typical phosphine−borane adducts. Interestingly, H4 on the phosphinine ring is shifted upfield by about 1 ppm (from 6.16 ppm in **10** to 5.19 ppm in **11**), which corroborates a higher partial charge on the ring. This anion was crystallized in the presence of [18]crown-6. It is a very rare example of a phosphine−borane adduct of an anion as only four such structures have been reported very recently.[36−39]As seen in Figure 3, the potassium atom is cryptated and coordinated to the BH_3 moiety via two of the three hydrogens. The two sulfur atoms show no interaction, and in fact, this species may be seen as a zwitterion. The central phosphorus is pyramidal (Σ angles P1 = 309.7°) and bound to the boron atom via a typical Lewis base−Lewis acid interaction (P1−B1 = 1.945(5) Å).

The very high coordination numbers accessible to f metal centers in particular prompted us to extend the methodology to the unknown tetradentate anionic derivatives. An example of a scorpionate-type ligand for which the pyridine was chosen as the fourth ligating moiety is presented here. In a first step the anion of 2-methyl pyridine was prepared via MeLi deprotonation and used without further purification.

Addition of this anion at low temperature on a solution of **1** followed by warming to room temperature led to formation of an orange solution (Scheme 6). The completeness of the reaction was checked by ^{31}P NMR spectroscopy. Compound **12** was then isolated in an excellent 91% yield by simple evaporation of the solvent, and it was fully characterized by NMR. In particular, it displays the "usual" set of triplet and doublet at −37.1 ppm ($^2J(P_A-P_B)$= 148.5 Hz) and at 43.1 ppm (PPh_2S) in the ^{31}P-{^{1}H} NMR spectrum, characteristic of the anions. Interestingly, the chemical shift of the central phosphorus atom at −37.1 ppm is similar to the one observed in other SPS$^{(R)}$ with bulky substituents. This data pointed to a long P−$C_{(subst)}$ bond which was later verified by X-ray crystallography. Notably, the methylene group bound to the pyridine appears as the expected

Scheme 6

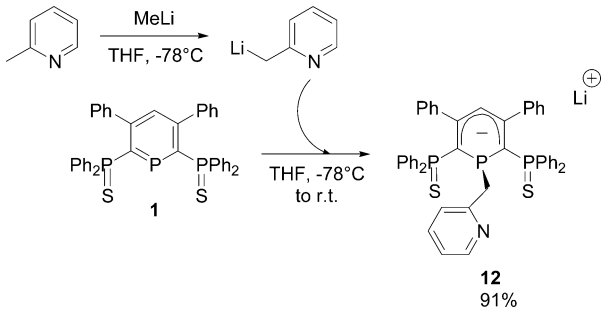

doublet at 3.36 ppm (^2J(H−P) = 2.5 Hz). The structure of **12** is presented in Figure 4 together with pertinent bond distances and angles. Unlike what was found by ^{31}P NMR spectroscopy for the liquid phase, the solid-state structure is unsymmetrical with only one sulfur atom bound to the lithium atom. The lithium center is tetracoordinated with one THF acting as the fourth ligand.

These examples clearly show the versatility of our synthesis, which allows the preparation of various anions. Optically pure substituents of tunable electronic properties may be introduced as well as an additional binding site.

Structural Studies and DFT Calculations on Lithium Complexes 2. As mentioned in the Introduction, an ambiguity subsisted in the description of the SPS$^{(R)}$ anions and either the delocalization of the charge from one sulfur to the other or localized on the central phosphorus atom was proposed. NMR data presented above already favor "Form A", but a thorough structural study was still warranted. One crystal structure of an anion has been reported, but it involved the OMe substituent at phosphorus,[24] whose electronic properties are very different from the alkyl-substituted anions. Two types of crystals were obtained for **2**: one, **2a**, from a sealed tube at −40 °C (mixture of THF/hexanes) and the other, **2b**, from slow diffusion of hexanes into a THF solution of the anion in a glovebox. These were solved by X-ray analysis, and the structures are presented in Figure 5.

In **2a** the anionic fragment acts as a tridentate pincer ligand for the lithium center, and a symmetrical coordination is observed (S1−Li and S2−Li 2.800(8) and 2.808(8) Å, respec-

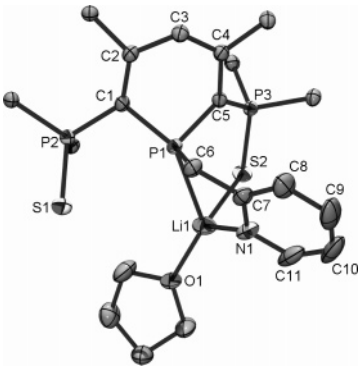

Figure 4. ORTEP plot (50% probability ellipsoids) of **12**. Phenyl groups are omitted. Bond distances (Å) and angles (deg): P1−C1 1.825(1), C1−C2 1.382(2), C2−C3 1.434(2), C3−C4 1.385(2), C4−C5 1.423(2), C5−P1 1.781(1), C6−P1 1.865(2), C1−P2 1.788(1), C5−P3 1.759(1), P2−S1 1.9735(5), P3−S2 1.9945(5), P1−Li1 2.482(3), S2−Li1 2.459(3), N1−Li1 2.071(4), O1−Li1 1.893(3), C1−P1−C5 100.22(7), P1−C1−C2 118.2(1), C1−C2−C3 122.3(1), C2−C3−C4 124.5(1), C3−C4−C5 122.1(1), C4−C5−P1 116.7(1), O1−Li1−N1 122.7(2), P1−Li1−N1 81.6(1), P1−Li1−S2 89.3(1), (mean plane C1−C2−C4−C5)−P1 22.8, (mean plane C1−C2−C4−C5)−C3 7.7, Σ angles P1 303.6.

(36) Izod, K.; McFarlane, W.; Tyson, B. V.; Clegg, W.; Harrington, R. W. *Chem. Commun.* **2004**, 570.
(37) Izod, K.; McFarlane, W.; Tyson, B. V.; Carr, I.; Clegg, W.; Harrington, R. W. *Organometallics* **2006**, *25*, 1135.
(38) Izod, K.; Wills, C.; Clegg, W.; Harrington, R. W. *Organometallics* **2006**, *25*, 38.
(39) Sun, X. M.; Manabe, K.; Lam, W. W. L.; Shiraishi, N.; Kobayashi, J.; Shiro, M.; Utsumi, H.; Kobayashi, S. *Chem.-Eur. J.* **2005**, *11*, 361.

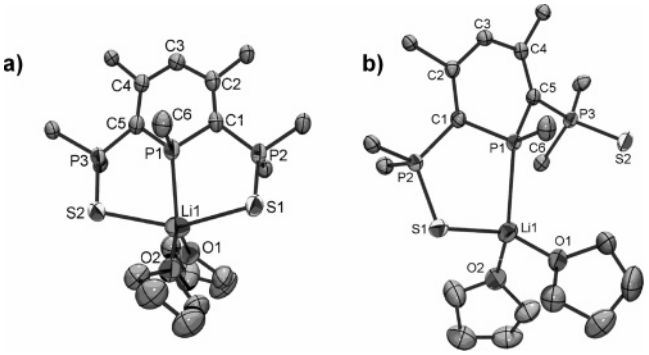

Figure 5. X-ray structure (50% probability ellipsoids) of **2**. Phenyl groups were omitted. (a) **2a** from sealed tube at −40 °C. (b) **2b** from slow diffusion. Structural parameters are given in Table 1.

tively). In **2b** only one sulfur atom is bound to the lithium center (S1−Li and S2−Li 2.469(3) and 4.559(3) Å). In both structures the phosphorus atom is bound to the Li atom in a η^1 fashion, with P−Li bond distances of 2.484(8) Å in **2a** and 2.600(4) Å in **2b**. This is in contrast with what was observed in the structures of monophosphinine anions (without ancillary ligands).[8] It is therefore shown once again that the presence of at least one ancillary ligand favors η^1 coordination of the phosphinine anions, as predicted and illustrated in the simple orbital diagram presented above. As already observed in the anion $SPS^{(OMe)}$, one major consequence of the nucleophilic attack is that the phosphinine ring is no longer planar. The P1 atom is located above a mean plane defined by the C1, C2, C4, and C5 atoms, and a dihedral angle of about 20° is measured (20.4° in **2a** and 21.1° in **2b**). Moreover, the phosphorus atom is now pyramidal, confirming the sp^3-type hybridization (Σ angles = 304.0° and 303.7° for **2a** and **2b**, respectively). The P1−C1 and P1−C5 bond distances of 1.821(1) Å in **2a** are much longer than in **1** (1.745(2) Å) and typical for a Psp^3-Csp^2 bond. The C3 atom is also located above the mean plane (dihedral angle of about 6°), and overall, the anion adopts a boat-like structure. The C−C bond distances of the ring are equivalent within the 3σ limit (1.389(5)−1.409(5) Å for **2a**), which proves the efficient delocalization of the charge over the five atoms of the ring. Moreover, the external P−C bond distances are significantly shortened in **2** (C1−P2 = 1.773(4) Å in **2a** vs 1.826(2) Å in **1**). Concomitantly, the P−S bonds are lengthened (P2−S1 = 1.974(4) Å in **2a** vs 1.956(1) Å in **1**). Only minor differences are observed in the structure of **2b**. Therefore, the structural data, in full agreement with the NMR data, are in favor of "Form A" with the negative charge being delocalized from one sulfur to the other. Nevertheless, nuances in this picture will appear resulting from the NBO analysis (vide supra). Because of the two different crystal structures of **2**, a ^{31}P NMR variable-temperature experiment was carried out in order to check if the unsymmetrical form (**2b**) could be observed by spectroscopy. In fact, only the symmetrical form is observed even down to −80 °C, which points to the very small difference in energy between these two species.

DFT calculations, using B3LYP at the 6-31+G* level of theory, were then carried out with the aim of quantifying this difference in energy. In a first step, model compounds $\mathbf{IIa_H}$ and $\mathbf{IIb_H}$, in which the phenyl groups were replaced by hydrogen atoms, were optimized. Interestingly, $\mathbf{IIb_H}$ was characterized as a minimum on the potential-energy surface, whereas a minimum for $\mathbf{IIa_H}$ could not be found. Thus, in a second step the steric crowding brought by the nine phenyl groups present in the real system was taken into account. The real complexes **IIa** and **IIb** were calculated using mixed quantum mechanics/molecular mechanics (QM/MM) at the ONIOM level[40] (B3PW91:UFF) with the phenyl groups in the MM part. The QM part was treated as above, and the MM was treated with the UFF. In order to quantify the difference in energy between the two systems, a single-point (B3PW91[41]) calculation was performed on the ONIOM-optimized geometries. **IIa** is lower in energy than **IIb** by a mere 1.6 kcal/mol. The potential-energy surface is thus very flat, which rationalizes the possible crystallization of two different structures, upon minor modification of the external conditions (temperature and solvent mixture).

NBO Analysis. Finally, a NBO analysis[42] was carried out on the model $\mathbf{I_H}$ (H replacing phenyl groups) of the neutral ligand **1** and models $\mathbf{IIb_H}$ (with the Li atom) and $\mathbf{III_H}$ (Li cation omitted) of anion **2**. This analysis was done on the geometry-optimized systems. Note that an excellent agreement between experimental and calculated structures was obtained (see Table 1 for comparison of structural parameters). One may note however that in the case of $\mathbf{III_H}$ omission of the Li cation naturally results in significant perturbation of the three bond distances involving the P of the ring.

Filled NBOs describe the different bonds or lone pairs that correspond to an idealized "strictly" localized Lewis structure. The real system deviates from this hypothetical structure because of donor−acceptor interactions between filled and empty NBOs. It thus provides a measure of the energetics of delocalization/hyperconjugation. The analysis of the neutral species $\mathbf{I_H}$ highlights several key points. First, the NBO charge at the phosphinine P1 atom is significantly higher (0.74) than what was previously calculated for other phosphinine species (below 0.7).[5] This is consistent with the higher reactivity of compound **1** toward weak nucleophiles such as alcohols. It is lower than the charge at the two P2 and P3 centers (0.826). Concomitantly, the charge at S1 and S2 is −0.544. NBO analysis confirms the structure of the phosphine sulfide as the expected hypervalent phosphorus moiety: a better description of compound **I** is therefore P^+-S^-, fully consistent with the sum of Wiberg bond indices at P of 4.05. In fact, NBO analysis gives three different lone pairs at the sulfur. The lowest one in energy is mainly an s orbital ($sp^{0.17}$), whereas the two others are almost degenerate pure p orbitals. These two lone pairs are stabilized via negative hyperconjugation into the two antibonding σ^*(P−H) and in the $\sigma^*(P-C_{ring})$ orbitals. This explains why the Wiberg bond index for the P−S bond is 1.4 and not 2 as in a "true" double bond (a Wiberg bond index of 1.96 is found in phosphaalkene HP=CH_2 for example). This hyperconjugation results in very significant stabilization of the sulfur lone pairs without involvement of P−S double-bond character. The resulting interaction energy can be estimated via either deletion of the appropriate off-diagonal elements of the Fock matrix in the NBO basis (E_{del} energy) or standard second-order perturbation approach (that affords a $E(2)$ energy). The magnitude of the donor−acceptor interaction is mainly controlled by (i) the energy gap (ΔE_{ij}) between the donor and acceptor orbitals, (ii) the corresponding Fock matrix element F_{ij}, and (iii) the occupation of the donor orbital n_i. As shown in Table 3, filled LP2(S) behaves as donor orbital and interacts with the two vicinal σ^*(P−H) (9.86 and 9.71 kcal/mol stabilization), whereas the filled LP3(S) interacts with the two vicinal σ^*(P−H) and σ^*(P−C) orbitals (2.83 and 16.09 kcal/mol, respectively). As expected for stereoelectronic effects, stabilization of the sulfur lone pairs by the vicinal

(40) Svensson, M.; Humbel, S.; Froese, R. D. J.; Matsubara, T.; Sieber, S.; Morokuma, K. *J. Phys. Chem.* **1996**, *100*, 19357.
(41) Becke, A. D. *J. Chem. Phys.* **1993**, *98*, 5648.
(42) Reed, A. E.; Curtiss, L. A.; Weinhold, F. *Chem. Rev.* **1988**, *88*, 899.

Table 1. Structural Parameters for SPS and [SPS^{Me}][Li(THF)$_2$]: X-ray Structures and Optimized Structures at the B3LYP/6-31+G* Level[a]

	I$_H$, DFT MQ	**1**, RX	**2a**, RX	**IIb$_H$**, DFT MQ	**2b**, RX	**III$_H$**, DFT MQ
P1−C2	1.751	1.742(2)	1.815(3)	1.821	1.811(2)	1.836
C2−C3	1.396	1.409(3)	1.389(5)	1.399	1.404(2)	1.392
C3−C4	1.398	1.399(3)	1.406(5)	1.401	1.397(2)	1.408
C4−C5	1.398	1.399(3)	1.409(5)	1.411	1.397(2)	1.408
C5−C6	1.396	1.417(3)	1.399(5)	1.389	1.390(2)	1.392
C6−P1	1.751	1.745(2)	1.802(4)	1.821	1.821(2)	1.836
P1−Me			1.835(4)	1.871	1.831(2)	1.880
C2−P2	1.848	1.826(2)	1.773(4)	1.765	1.766(2)	1.775
C6−P3	1.848	1.835(2)	1.782(1)	1.783	1.779(2)	1.775
P2−S1	1.963	1.956(1)	1.974(4)	2.019	1.9887(6)	1.999
P3−S2	1.963	1.9532(8)	1.981(1)	1.989	1.9678(6)	1.999
P1−Li			2.484(8)	2.573	2.600(3)	
S1−Li			2.800(8)	2.499	2.469(3)	
S2−Li			2.820(8)	4.343	4.599(3)	
P1−C2−C3	124.6	118.2(1)	118.7(3)	121.4	118.2(1)	121.8
C2−C3−C4	123.4	121.0(2)	123.1(3)	124.5	122.9(1)	125.1
C3−C4−C5	122.2	127.9(2)	124.8(3)	121.5	125.9(1)	121.1
C4−C5−C6	123.1	120.4(2)	122.3(3)	125.4	121.8(1)	125.1
C5−C6−P1	124.7	123.3(2)	118.9(3)	120.7	118.7(1)	121.8
C6−P1−C2	100.8	103.9(1)	100.3(2)	98.2	100.27(7)	96.5
Pyram. P1			304.0	303.9	303.7	299.6

[a] Distances are in Angstroms and angles in degrees.

Table 2. NBO Charges, Wiberg Bond Indices, and ΣWiberg Bond Indices

	I_H	IIb_H	IIb_H	III_H
NBO charges				
q_{P1}	0.744	0.793		0.842
q_{P2}/q_{P3}	0.826	0.912	0.890	0.882
q_{S1}/q_{S2}	−0.544	−0.711	−0.646	−0.682
q_{Li}		0.826		
Wiberg bond indices				
n(P−H) (P_2/P_3)	0.872	0.867	0.891	0.879
n(P−H) (P_2/P_3)	0.872	0.862	0.879	0.879
n(P−S) (P_2/P_3)	1.418	1.222	1.316	1.292
n(P−C) (P_2/P_3)	0.840	0.982	0.934	0.954
n(P1−C)	1.290	0.932		0.921
n(P1−C)	1.290	0.923		0.921
n(P1−Me)		0.895		0.891
n(S−Li)		0.089	0.009	
n(P1−Li)		0.097		
Σ Wiberg bond indices				
at P1	2.88	3.06		2.92
at P2/P3	4.05	4.04	4.06	4.08
at S	1.76	1.59	1.65	1.63

Table 3. NBO Analysis of Hyperconjugative Interactions in Neutral I$_H$

donor orbital	acceptor orbital	$E(2)$ kcal/mol	ΔE_{ij} (au)	F_{ij} (au)
neutral **I$_H$**				
LP2(S) p	σ^*(P−H_{11})	9.71	0.40	0.057
LP2(S) p	σ^*(P−H_{12})	9.86	0.40	0.057
LP3(S) p	σ^*(P−C)	16.09	0.35	0.068
LP3(S) p	σ^*(P−H_{11})	2.98	0.40	0.032
LP3(S) p	σ^*(P−H_{12})	2.83	0.40	0.031
III$_H$ (for one monomer)				
LP2(S) p	σ^*(P−C)	1.57	0.42	0.023
LP2(S) p	σ^*(P−H_{11})	10.97	0.41	0.061
LP2(S) p	σ^*(P−H_{12})	4.56	0.40	0.039
LP3(S) p	σ^*(P−C)	11.17	0.42	0.062
LP3(S) p	σ^*(P−H_{11})	<0.5		
LP3(S) p	σ^*(P−H_{12})	7.02	0.42	0.048

antibonding σ^* orbitals strongly depends on the relative orientation of the donor/acceptor orbitals (schematically presented in Figure 7, left-hand side). Therefore, the total stabilization of the lone pairs at each sulfur atom amounts to about 38.6 (19.57 kcal/mol for LP2(S) and 19.07 kcal/mol for LP3(S)). Importantly, for the purpose of comparison with the anion (vide supra), donation of part of the sulfur lone pair electronic densities into the σ^*(P−C_{ring}) reduces this latter Wiberg bond index, which is therefore lower than the expected value of 1.0 (typical for single bond) at 0.840. Similarly, the Wiberg bond index of the two P−H bonds is 0.872. On the other hand, the Wiberg bond indices for the two P−C bonds (intraring) of the phosphinine are 1.29, close to the expected 1.5 for a delocalized system (like in benzene).

Significant structural modifications arise from formation of anion **2** upon addition of MeLi on this neutral species. In terms of NBO analysis, one finds three single bonds at P1 with the newly formed P−Me having a slightly lower bond index, correlated with a slightly longer bond distance (see Table 1). As expected, the NBO analysis indicates that the S−Li and P−Li interactions are essentially electrostatic in nature ($n_{Wiberg} < 0.1$, $q_{Li} > 0.8$). The next question to be answered concerns

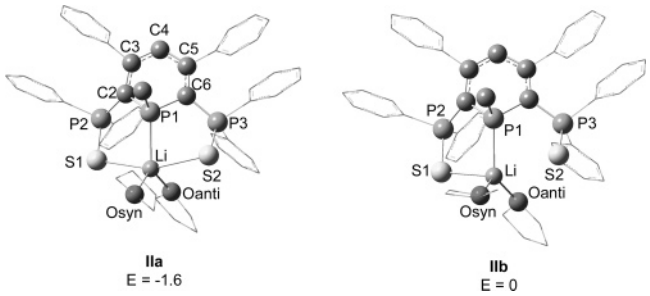

Figure 6. Optimized structures of **IIa** and **IIb** at the ONIOM (B3PW91:UFF) level. MQ (MM) is represented with balls (sticks). Structural parameters are found in Table 1; E = relative energies in kcal·mol^{-1}.

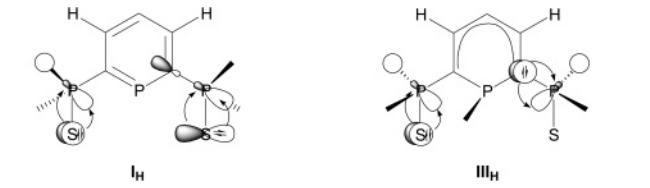

Figure 7. Principal donor−acceptor interactions in **I$_H$** and **III$_H$**. The "competition" for the acceptor fragments in the anion is represented.

Scheme 7

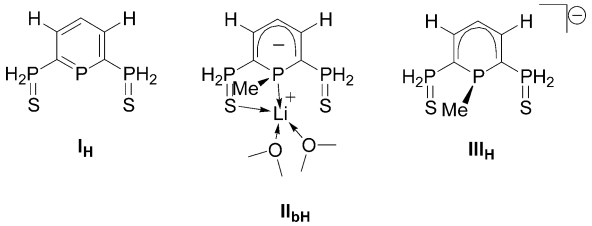

Scheme 8

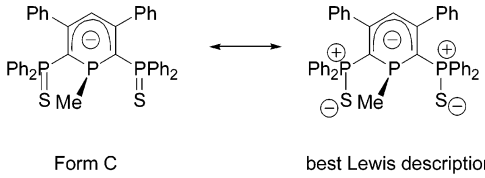

the way the additional charge is stabilized. We have shown recently that two phosphine sulfide moieties were able to stabilize not only a negative charge in the α position but also a geminal dianion via negative hyperconjugation. In the present case, each phosphine sulfide will have to stabilize only a partial charge located on each α carbon of the ring. Clearly, this partial charge located in a p orbital at carbon will compete with the lone pairs (p orbitals) at S to be stabilized by the two antibonding σ^*(P−H) orbitals (Figure 7, right-hand side). For the sake of simplicity in the description, we will focus on the modification of the stabilization of the sulfur lone pairs, which is directly related to the partial charge at carbon. Both models with and without Li were computed and showed very minor differences linked to the loss of symmetry in the system (see Table 1). Therefore, from now on we will focus on the symmetrical compound $\mathbf{III_H}$. Very significantly, although the Wiberg bond index for the two P−H bonds is hardly modified, the index for P−S decreases. This is traced back to the decreased electron transfer from the S lone pairs, consistent with an increased charge at S in the anion (−0.682 vs −0.544 in neutral).

As shown in Table 3, the overall stabilization to the two sulfur lone pairs by the two vicinal σ^*(P−H) and σ^*(P−C) orbitals is reduced to 16.8 and 18.2 kcal/mol, respectively (total of 35.0 vs 38.6 kcal/mol in $\mathbf{I_H}$). This points to a significant stabilization of the added charge on each PH_2S fragment by about 3.6 kcal/mol (total 7.2 kcal/mol). Overall, the NBO analysis reveals that the anionic system is best described as a "Form C" drawn in Scheme 8, namely, a phosphacyclohexadienyl anion stabilized by negative hyperconjugation into the two PS pendant arms. In this representation the anionic charge is stabilized by both delocalization over the five carbon atoms *and* negative hyperconjugation and not as in "Form A" as a fully delocalized charge from one S to the other.

Conclusion

We synthesized a wide range of $SPS^{(R)}$ anionic ligands from a single precursor SPS among which are the first examples of a potentially tetradentate SPSN anionic ligand and optically pure derivatives. Several anions were crystallized which allowed a precise structural analysis of these species, which proves that the sp^2-hybridized P center of the starting compound is transformed into a sp^3 phosphorus center. The central moiety was thus shown to be a "classical" phosphine. NBO analysis then revealed how the added charge is accommodated on the system, namely, both by delocalization over the five carbon atoms of the cycle (pentadienyl like structure) *and* by negative hyperconjugation in the two PPh_2S pendant arms. This latter stabilization is reminiscent of the stabilization of phosphorus ylides. The precise electronic description is therefore "Form C" drawn above.

Experimental Section

General. All reactions were routinely performed under an inert atmosphere of argon or nitrogen using Schlenk and glovebox techniques and dry deoxygenated solvents. Dry THF, hexanes, and diethyl ether were obtained by distillation from Na/benzophenone and dry CH_2Cl_2 from P_2O_5. $CDCl_3$ was dried from P_2O_5 and stored on 4 Å Linde molecular sieves. CD_2Cl_2 was used as purchased and stored in the glovebox. Nuclear magnetic resonance spectra were recorded on a Bruker AC-200 SY spectrometer operating at 300.0 MHz for ^{1}H, 75.5 MHz for ^{13}C, and 121.5 MHz for ^{31}P. Solvent peaks are used as an internal reference relative to Me_4Si for ^{1}H and ^{13}C chemical shifts (ppm); ^{31}P chemical shifts are relative to a 85% H_3PO_4 external reference. Coupling constants are given in Hertz. The following abbreviations are used: s, singlet; d, doublet; t, triplet; q, quadruplet; p, pentuplet; m, multiplet; v, virtual; b, broad. Mass spectra were obtained at 70 eV with a HP 5989B spectrometer coupled to a HP 5980 chromatograph by the direct inlet method. Phosphinine **1** and solutions of (−)-menthyl grignard reagent[27] and Li−methyl pyridine[43] were prepared according to reported procedures.

$[SPS^{(Me)}][Li(THF)_2]$, 2. To a stirred solution of **1** (200 mg, 0.29 mmol) in THF (10 mL) at −78 °C was added MeLi in diethyl ether (1.8 mL, C = 0.16 M, 0.29 mmol). The mixture was then warmed to room temperature and stirred for an additional 20 min. The initially colorless solution turned instantaneously deep red. After solvent evaporation, the title compound **2** was obtained as a red solid, highly sensitive to hydrolysis. Yield: 245 mg (100%). Crystals were grown by two different methods: from THF/hexanes solution of **2** in a sealed tube at −40 °C (structure **2a**) and from slow diffusion of hexanes into a THF solution of **2** in a glove box (structure **2b**). Compound **2** is too sensitive to hydrolysis to obtain a satisfactory elemental analysis.

^{1}H NMR (THF-d_8): δ 0.99 (d, ^2J(H−P_A) = 3.4, 3H, CH_3), 5.13 (t, ^4J(H−P_B) = 4.8, 1H, H_4), 6.53−7.57 (m, 30H, CH of Ph).

^{13}C NMR (THF-d_8): δ 10.6 (dt, ^1J(C−P_A) = 17.2, ^3J(C−P_B) = 5.8, CH_3), 73.6 (ddd, ^1J(C−P_A) = 83.9, ^1J(C−P_B) = 6.0, ^3J(C−$P_{B'}$) = 2.7, $C_{2,6}$), 119.9 (t, ^3J(C−P_B) = 11.8, C_4), 126.6−133.6 (m, 9 × CH of Ph), 140.3 (d, ^1J(C−P_B) = 81.1, C of PPh_2), 140.7 (d, ^1J(C−P_B) = 83.1, C of PPh_2), 146.1 (m, Σ J(C−P) = 8.4, $C_{3,5}$), 155.2 (m, Σ J(C−P) = 11.0, C of Ph).

^{31}P NMR (THF-d_8): δ 45.9 (d, ^2J(P_A−P_B) = 155.5, P_BPh_2), −65.7 (t, ^2J(P_A−P_B) = 155.5, P_AMe).

$[SPS^{Bu}][Li(THF)_2]$, 3. A similar procedure was used to synthesize **3** from **1** using a stoichiometric amount of BuLi. The title compound was obtained as a red powder. Yield: 100%. Compound **3** is too sensitive to hydrolysis to obtain a satisfactory elemental analysis.

^{1}H NMR (THF-d_8): δ 1.08 (t, ^3J(H−H) = 7.5, 3H, CH_3), 1.20−2.26 (m, 6H CH_2), 5.32 (t, ^4J(H−P_B) = 4.6, 1H, H_4), 6.68−7.77 (m, 30H, CH of Ph).

^{13}C NMR (THF-d_8): δ 11.9 (s, CH_3), 23.7 (s, CH_2), 30.2 (s, CH_2), 35.7 (m, CH_2−P), 71.9 (ddd, ^1J(C−P_A) = 81.8, ^1J(C−P_B) = 5.7, ^3J(C−P_B) = 3.3, $C_{2,6}$), 120.8 (t, ^3J(C−P_B) = 11.3, C_4), 126.6−133.6 (m, CH of Ph), 139.5 (d, ^{1}J(C−P_B) = 80.7, C of PPh_2), 141.0 (d, ^{1}J(C−P_B) = 83.1, C of PPh_2), 145.9 (m, ΣJ(C−P) = 6.9, $C_{3,5}$), 155.8 (m, Σ J(C−P) = 9.6, C of Ph).

^{31}P NMR (THF-d_8): δ 45.8 (d, ^2J(P_A−P_B) = 156.0, P_BPh_2), −66.2 (t, ^2J(P_A−P_B) = 156.0, P_ABu).

(43) Fraser, R. R.; Mansour, T. S.; Savard, S. *J. .Org. Chem.* **1985**, *50*, 3232.

[SPS$^{(t-Bu)}$][Li(THF)$_2$], 4. To a stirred solution of **1** (40 mg, 0.06 mmol) in THF-d_8 (10 mL) at −78 °C was added *t*-BuLi in pentane (40 μL, C = 1.5 M, 0.06 mmol). The mixture was then warmed to room temperature and stirred for an additional 2 min. The initially colorless solution turned instantaneously deep red. Compound **4** was observed as an intermediate and could not be isolated.

^{1}H NMR (THF-d_8) (selected data): δ 5.20 (t, ^4J(H−P$_B$) = 4.0, 1H, H$_4$).

^{31}P NMR (THF-d_8): δ 46.2 (d, ^2J(P$_A$−P$_B$) = 158.0, P$_B$Ph$_2$), −43.1 (t, ^2J(P$_A$−P$_B$) = 158.0, P$_A$*t*-Bu).

[SPS$^{(H)}$][Li(THF)$_2$], 5. To a stirred solution of **1** (200 mg, 0.29 mmol) in THF (10 mL) at −78 °C was added *t*-BuLi in pentane (193 μL, C = 1.5 M, 0.29 mmol). The mixture was then warmed to room temperature and stirred for an additional 20 min. The initially colorless solution turned instantaneously deep red. Compound **5** was stable in solution but decomposed when dried. The reaction was thus performed in THF-d_8 to obtain NMR data. NMR yield: 100%.

^{1}H NMR (THF-d_8): δ 4.41 (dt, ^1J(H−P$_A$) = 195.8, ^3J(H−P$_B$) = 15.0, 1H, P−H), 5.59 (t, ^4J(H−P$_B$) = 5.2, 1H, H$_4$), 6.70−7.91 (m, 30H, CH of Ph).

^{13}C NMR (THF-d_8): δ 66.2 (m, C$_{2,6}$), 122.1 (t, ^3J(C−P$_B$) = 12.0, C$_4$), 126.6−133.8 (m, 9 × CH of Ph), 139.7 (dd, ^1J(C−P$_B$) = 81.1, ^3J(C−P$_A$) = 1.5, C of Ph), 140.0 (dd, ^1J(C−P$_B$) = 83.7, ^3J(C−P$_A$) = 3.3, C of Ph), 146.0 (d, J(C−P) = 5.5, C$_{3,5}$), 160.0 (d, ^3J(C−P$_A$) = 7.0, C of Ph).

^{31}P NMR (THF-d_8): δ −73.7 (dt, ^1J(P$_A$−H) = 195.8, ^2J(P$_A$−P$_B$) = 148.2, P$_A$H), 43.2 (d, ^2J(P$_A$−P$_B$) = 148.2, P$_B$Ph$_2$).

[SPS$^{(OMen)}$][Li(THF)$_2$], 6. To a stirred solution of **1** (150 mg, 0.22 mmol) in THF (5 mL) was added Li−mentholate (35.7 mg, 0.66 mmol). The mixture was stirred 15 min at room temperature. After evaporation of the solvent, **6** was obtained as a yellow powder. NMR yield: 100%. Compound **6** was too sensitive to hydrolysis to obtain a satisfactory elemental analysis.

^{31}P NMR (THF-d_8): δ 45.1 (AXX′, d, ^2J(P$_X$−P$_A$) = 171.6, P$_X$-Ph$_2$), 45.4 (AXX′, d, ^2J(P$_{X'}$−P$_A$) = 176.2, P$_{X'}$Ph$_2$), 61.8 (pseudo t, d, ^2J(P$_X$−P$_A$) = ^2J(P$_{X'}$−P$_A$) = 176.9, P$_A$−OMen).

[SPS$^{(Men)}$][MgCl], 7. To a stirred solution of **1** (100 mg, 0.15 mmol) in THF (5 mL) at −78 °C was added an excess of a THF solution of (−)-MenMgCl (0.64 mL, C = 0.46 M, 0.30 mmol). The mixture was then warmed to room temperature and stirred for an additional 1 h. The initially colorless solution slowly turned deep red and was extremely viscous. NMR yield: 100%.

^{31}P NMR (THF-d_8): δ −38.7 to −35.4 (ABB′, m, P$_A$Men), 42.1−44.3 (ABB′, m, PPh$_2$).

λ^5-Phosphinine 8a, 1,2-Dihydrophosphinine 8b, and 1,4-Dihydrophosphinine 8c. To the viscous mixture of 7 obtained as above EtOH was added (60 μL, 1 mmol). The solution was stirred for 20 min. Complete formation of 1,1-λ^5-phosphinine 8a was verified by ^{31}P NMR. After evaporation, the solid was redissolved in CH_2Cl_2 and filtered rapidly through a pad of silica gel. After evaporation, 8a was obtained as a yellow powder. Yield: 214 mg (87%). In solution, 8a isomerized partially into 8b and 8c within 30 min.

8a. ^{1}H NMR (C_6D_6): δ 1.04 (d, ^3J(H−H) = 6.9, 3H, CH$_3$), 1.07 (t, ^3J(H−H) = 6.6, 3H, CH$_3$), 1.19−1.27 (m, 3H), 1.39 (s, 3H, CH$_3$), 1.56−1.98 (m, 3H, CH and CH$_2$), 2.21 (m, 1H, CH), 3.54 (m, 2H), 3.31 (m, 1H, CH), 5.73 (pseudo t, ^4J(P$_B$−H) = ^4J(P$_{B'}$−H) = 3.8, 1H, H$_4$), 6.74−7.04 (m, 17H, CH of Ph), 7.39−7.49 (m, 3H, CH of Ph), 7.73−7.85 (m, 5H, CH of Ph), 8.18−8.29 (m, 5H, CH of Ph), 8.63 (d pseudo t, ^1J(P$_A$−H) = 493.9, ^4J(P$_B$−H) = ^4J(P$_{B'}$−H) = 5.5, 1H, P−H)

^{31}P NMR (C_6D_6): δ −6.3 (AXX′, d pseudo t, ^1J(P$_A$−H) = 493.9, ^2J(P$_A$−P$_X$) = 40.0, P$_A$Men), 38.7 (AXX′, d, ^2J(P$_A$−P$_X$) = 39.2, P$_X$Ph$_2$), 38.7 (AXX′, d, ^2J(P$_A$−P$_X$) = 41.8, P$_{X'}$Ph$_2$).

8b. ^{31}P NMR (C_6D_6): δ −55.3 (AXX′, dd, ^2J(P$_A$−P$_X$) = 127.6, ^2J(P$_A$−P$_{X'}$) = 109.4, P$_A$Men), 40.8 (AXX′, d, ^2J(P$_A$−P$_X$) = 127.6, P$_X$Ph$_2$), 44.1 (AXX′, d, ^2J(P$_A$−P$_X$) = 109.4, P$_{X'}$Ph$_2$).

8c. ^{31}P NMR (C_6D_6): δ −53.9 (AXX′, pseudo t, ^2J(P$_A$−P$_X$) = ^2J(P$_A$−P$_{X'}$) = 120.3, P$_A$Men), 39.9 (AXX′, d, ^2J(P$_A$−P$_X$) = 122.3, P$_X$Ph$_2$), 43.6 (AXX′, d, ^2J(P$_A$−P$_{X'}$) = 117.1, P$_{X'}$Ph$_2$).

[SPS$^{(Men)}$][Li(THF)$_2$], 9. To a stirred solution of a mixture of **8a**−**c** (200 mg, 0.24 mmol) in THF (10 mL) at −78 °C was added MeLi in diethyl ether (0.182 mL, C = 1.6 M, 0.29 mmol). The mixture was then warmed to room temperature and stirred for an additional 20 min. The initially yellow solution turned instantaneously deep red. After evaporation, **9** was obtained as a red powder. NMR yield: 100%. Compound **9** was too sensitive to hydrolysis to obtain a satisfactory elemental analysis.

^{31}P NMR (THF-d_8):δ −45.1 (ABB′, pseudo t, ^2J(P$_A$−P$_B$) = ^2J(P$_A$−P$_{B'}$) = 154.3, P$_A$Me), 43.1 (ABB′, d, ^2J(P$_A$−P$_B$) = 159.2, P$_B$Ph$_2$), 43.7 (ABB′, d, ^2J(P$_A$−P$_B$) = 153.1, P$_{B'}$Ph$_2$).

[SPS$^{(Me)}$][K(THF)$_2$], 10. In a glovebox, **2** (150 mg, 0.18 mmol) and *t*-BuOK (21 mg, 0.185 mmol) were weighed and placed in a Schlenk flask. Outside the box, diethyl ether (20 mL), cooled to −78 °C, was slowly canulated in the flask containing the solids (at −78 °C). The mixture was stirred for 4 h at this temperature, which was then allowed to warm back to room temperature overnight. An orange solid precipitated. In a glovebox the mixture was transferred into tubes and centrifuged for 5 min. The solid was rinsed twice with diethyl ether and centrifuged each time. The solid was dissolved in THF (20 mL), transferred to a Schlenk flask, and taken to dryness. The title compound **10** was obtained as an orange solid in 89% yield. Crystals suitable for X-ray analysis were grown by slow diffusion of hexanes in a THF solution of **10** in the glovebox. Compound **10** was too sensitive to hydrolysis to obtain a satisfactory elemental analysis.

^{1}H NMR (THF-d_8): δ 1.14 (d, ^2J(H−P$_A$) = 5.1, 3H, CH$_3$), 1.79 (bs, CH$_2$), 3.65 (bs, CH$_2$), 5.36 (t, ^4J(H−P$_B$) = 5.1, 1H, H$_4$), 6.69−8.02 (m, 30H, CH of Ph).

^{13}C NMR (THF-d_8): δ 10.2 (dt, ^1J(C−P$_A$) = 20.4, ^3J(C−P$_B$) = 4.6, CH$_3$), 26.5 (s, CH$_2$), 68.4 (s, CH$_2$), 74.8 (ddd, ^1J(C−P$_A$) = 87.6, ^1J(C−P$_B$) = 13.3, ^3J(C−P$_{B'}$) = 7.1, C$_{2,6}$), 118.6 (t, ^3J(C−P$_B$) = 12.0, C$_4$), 126.6 (s, CH of Ph), 127.4 (s, CH of Ph), 127.7 (d, J(C−P) = 11.9, CH of Ph), 128.2 (d, J(C−P) = 11.7, CH of Ph), 129.4 (d, J(C−P) = 2.7, CH of Ph), 130.1 (d, J(C−P) = 2.7, CH of Ph), 130.6 (s, CH of Ph), 133.1 (d, J(C−P) = 10.3, CH of Ph), 133.5 (d, J(C−P) = 10.4, CH of Ph), 140.7 (dd, ^1J(C−P$_B$) = 79.3, ^1J(C−P$_A$) = 2.9, C of Ph), 141.8 (d, ^1J(C−P) = 83.0, CH of Ph), 146.4 (d, J(C−P) = 6.0, C$_{3,5}$), 154.5 (dd, J(C−P) = 7.4, J(C−P) = 2.6, C of Ph).

^{31}P NMR (THF-d_8): δ −62.0 (t, ^2J(P$_A$−P$_B$) = 151.9, P$_A$Me), 43.1 (d, ^2J(P$_A$−P$_B$) = 155.9, P$_A$Ph$_2$).

[SPS$^{(Me)}$·BH$_3$][K(Et$_2$O)$_{0.5}$], 11. In the glovebox THF (50 mL) was added to [SPS$^{(Me)}$][K(Et$_2$O)] (210 mg, 0.260 mmol) in a flask, and 1.3 equiv of BH$_3$·Me$_2$S (2.0 M) solution in diethyl ether (169 μL, 0.338 mmol) was introduced via a syringe. The reaction mixture was stirred for 4 h at 20 °C. After evaporation and drying under vacuum, the residue was recrystallized with diethyl ether (40 mL). The microcrystalline orange powder was filtered and dried under vacuum. Yield: 184.4 mg (90.4%)

^{1}H NMR (THF-d_8) δ = −0.06 [bs, $w_{1/2}$ = 170 Hz, 3H, BH$_3$], 1.30 [d, ^2J(H−P$_A$) = 9.0, 3H, CH$_3$], 5.19 [t, ^4J(H−PB) = 4.8, 1H, H^4], 6.65−8.21 (m, 30H, CH of Ph).

^{31}P NMR (THF-d_8): δ = 37.39 [AB$_2$, d, ^2J(PA−PB) = 60, P$_B$], 2.87 [bs, $w_{1/2}$ = 165 Hz, BH$_3$P$_A$Me].

^{11}B NMR (THF-d_8): δ = −37.3 [bs, $w_{1/2}$ = 290 Hz, BH$_3$].

Crystals of [SPS$^{(Me)}$·BH$_3$][K(^{18}crown-6)(THF)] suitable for X-ray analysis were grown by addition of [18]crown-6 over a THF solution of [SPS$^{(Me)}$·BH$_3$][K(Et$_2$O)$_{0.5}$].

[SPS$^{(CH2Py)}$][Li(THF)$_2$], 12. In a glovebox a solution of Li−methyl pyridine (237 μL, C = 0.62 M, 0.15 mmol) was added via a microsyringe to a solution of phosphinine **1** (100 mg, 0.15 mmol) in THF (3 mL). The resulting mixture was stirred at room temperature for 10 min. After evaporation of the solvent, compound

Table 4. Experimental Details for X-ray Crystal Structures of 2a and 2b

	2a	2b
cryst size (mm)	0.20 × 0.20 × 0.20	0.22 × 0.18 × 0.18
empirical formula	$C_{58}H_{66}LiO_4P_3S_2$	$C_{50}H_{50}LiO_2P_3S_2$
mol wt	991.08	846.87
cryst syst	triclinic	triclinic
space group	$P\bar{1}$	$P\bar{1}$
a (Å)	12.428(1)	10.565(1)
b (Å)	17.843(1)	13.316(1)
c (Å)	24.445(1)	17.546(1)
α (deg)	77.010(1)	73.077(1)
β (deg)	87.640(1)	74.380(1)
γ (deg)	89.450(1)	75.770(1)
V (Å^3)	5277.5(6)	2236.5(3)
Z	4	2
calcd density (g cm^{-3})	1.247	1.258
abs coeff (cm^{-1})	0.238	0.265
2*θ* max (deg)	48.22	54.96
F(000)	2104	892
index ranges	−14 to +14; −20 to +20; −25 to +28	−13 to +13; −17 to +17; −22 to +22
no. of collected/indep reflns	26 699/16 562	15 496/10 204
no. of reflns used	11 710	8291
R_{int}	0.0289	0.0156
abs cor	multiple scans; 0.9540 min, 0.9540 max	multiple scans; 0.9439 min, 0.9538 max
no. of params refined	1242	528
no. of reflns/params	9	15
final R1[a]/wR2 ($I > 2\sigma(I)$)[b]	0.0611/0.1783	0.0383/0.1053
goodness of fit on F^2	1.025	1.069
diff peak/hole (e Å^{-3})	0.823(0.061)/−0.499(0.061)	0.334(0.047)/−0.315(0.047)

[a] $R1 = \Sigma||F_o| - |F_c||/\Sigma|F_o|$. [b] $wR2 = (\Sigma w||F_o| - |F_c||^2/\Sigma w|F_o|^2)^{1/2}$.

Table 5. Experimental Details for X-ray Crystal Structures of 10, 11, and 12

	10	11	12
cryst size (mm)	0.20 × 0.18 × 0.15	0.35 × 0.25 × 0.10	0.22 × 0.22 × 0.20
empirical formula	$C_{50}H_{50}KO_2P_3S_2$	$C_{42}H_{37}BP_3S_2$,$C_{16}H_{32}KO_7$, C_4O	$C_{51}H_{45}LiNOP_3S_2$
mol wt	879.03	1157.18	851.85
cryst syst	triclinic	monoclinic	monoclinic
space group	$P\bar{1}$	$P2_1/m$	$P2_1/c$
a (Å)	12.324(1)	9.3537(2)	13.737(1)
b (Å)	13.105(1)	20.6676(6)	12.366(1)
c (Å)	15.844(1)	15.8981(7)	26.453(1)
α (deg)	74.112(1)		
β (deg)	68.143(1)	93.302(1)	104.747(1)
γ (deg)	86.087(1)		
V (Å^3)	2282.6(3)	3068.30(17)	4345.6(5)
Z	2	2	4
calcd density (g cm^{-3})	1.279	1.253	1.302
abs coeff (cm^{-1})	0.352	0.285	0.273
2*θ* max (deg)	60	51.36	60
F(000)	924	1228	1784
index ranges	−17 to +16; −17 to +18; −22 to +22	0 to +11; 0 to +25; −19 to +19	−19 to +18; −15 to +17; −37 to +25
no. of collected/indep reflns	19 152/13 220	5987/5987	68 403/12 572
no. of reflns used	9480	5068	9396
R_{int}	0.0183	0.0627	0.0327
abs cor	multiscan; 0.9330 min, 0.9491 max	none	multiscan; 0.9424 min, 0.9475 max
no. of params refined	564	373	536
no. of reflns/params	16	13	17
final R1[a]/wR2 ($I > 2\sigma(I)$)[b]	0.0486/0.1471	0.0558/0.1619	0.0392/0.1058
goodness of fit on F^2	1.092	1.057	1.002
diff peak/hole (e Å^{-3})	0.659(0.065)/−0.610(0.065)	1.140(0.079)/−0.761(0.079)	0.380(0.055)/−0.308(0.055)

[a] $R1 = \Sigma||F_o| - |F_c||/\Sigma|F_o|$. [b] $wR2 = (\Sigma w||F_o| - |F_c||^2/\Sigma w|F_o|^2)^{1/2}$.

12 was obtained as an orange powder. Crystals suitable for X-ray crystal structure analysis were grown by diffusion of hexanes into a concentrated solution of **12** in THF. Yield: 116 mg (91%). Compound **12** was too sensitive to hydrolysis to obtain a satisfactory elemental analysis.

^{1}H NMR (THF-d_8): δ 3.36 (d, ^2J(H−P) = 2.5, 2H, CH_2), 5.41 (t, ^4J(H−P) = 5.0, 1H, H_4), 6.73−7.03 (m, 12H, CH of Ph), 7.15−7.49 (m, 15H, 1H of Py and 14H of Ph), 7.47 (d, ^3J(H−H) = 7.7, CH of Py), 7.70 (td, ^3J(H−H) = 7.7, ^5J(H−H) = 1.9, 1H, CH of Py), 8.00 (dd, J(H−P) = 12.6, J(H−H) = 7.8, 4H, CH of Ph), 8.44 (d, J(H−H) = 5.3, 1H, CH of Py).

^{13}C NMR (THF-d_8): δ 38.3 (d, ^1J(C−P) = 32.7, CH_2), 74.6 (ddd, ^1J(C−P) = 87.2, ^1J(C−P) = 18.9, ^3J(C−P) = 7.2, $C_{2,6}$), 120.8 (t, ^3J(C−P) = 11.9, C_4H), 122.2 (d, J(C−P) = 1.5, CH of Py), 128.0 (s, CH of Ph), 128.2 (d, J(C−P) = 2.5, CH of Py), 128.5 (s, CH of Ph), 128.7 (d, J(C−P) = 12.1, CH of Ph), 129.1 (d, J(C−P) = 12.1, CH of Ph), 130.4 (d, J(C−P) = 2.5, CH of Ph), 131.2 (d, J(C−P) = 2.4, CH of Ph), 133.9 (d, J(C−P) = 10.4, CH of Ph), 134.7 (dd, J(C−P) = 10.4, J(C−P) = 2.0, CH of Ph), 138.9 (s, CH of Py), 141.3 (dd, J(C−P) = 86.1, J(C−P) = 4.9, C of Ph), 141.5 (dd, J(C−P) = 74.2, J(C−P) = 1.1, C of Ph), 146.9 (dd, J(C−P) = 5.1, J(C−P) = 2.4, C of Ph or $C_{3,5}$), 150.2 (s, CH of

Py), 156.9 (dd, $J(C-P) = 6.7$, $J(C-P) = 2.9$, C of Ph or $C_{3,5}$), 163.5 (d, $^2J(C-P) = 5.3$, C ofde Py).

^{31}P NMR (THF-d_8): δ −37.1 (t, $^2J(P_A-P_B)= 148.5$, P_A), 43.1 (d, $^2J(P_A-P_B)= 148.5$, P_BPh_2).

X-ray Crystallographic Study. Data were collected at 150.0(1) K on a Nonius Kappa CCD diffractometer using a Mo Kα (λ = 0.71070 Å) X-ray source and a graphite monochromator. All data were measured using phi and omega scans. Experimental details are described in Tables 4 and 5. The crystal structures were solved using SIR 97[44] and Shelxl-97.[45] ORTEP drawings were made using ORTEP III for Windows.[46] CCDC-646623 to 646627 contain the supplementary crystallographic data for this paper. These data can be obtained free of charge at www.ccdc.cam.ac.uk/conts/retrieving.html or from the Cambridge Crystallographic Data Centre, 12, Union Road, Cambridge CB2 1EZ, UK; fax: (internat.) +44−1223/336−033; E-mail: deposit@ccdc.cam.ac.uk

(44) Altomare, A.; Burla, M. C.; Camalli, M.; Cascarano, G.; Giacovazzo, C.; Guagliardi, A.; Moliterni, A. G. G.; Polidori, G.; Spagna, R. *SIR97, an integrated package of computer programs for the solution and refinement of crystal structures using single crystal data.*

(45) Sheldrick, G. M. *SHELXL-97;* Universität Göttingen: Göttingen, Germany, 1997.

(46) Farrugia, L. J. *ORTEP-3;* Department of Chemistry, University of Glasgow.

Acknowledgment. This work was supported by the CNRS, the Ecole Polytechnique, and the DGA. M.D. thanks the DGA for financial support. The authors would like to thank IDRIS (Paris XI Orsay University) for the allowance of computer time.

Supporting Information Available: Computed Cartesian coordinates, SCF energies, thermochemistry, and three lower frequencies of the theoretical structures $\mathbf{I_H}$, $\mathbf{IIb_H}$, and $\mathbf{III_H}$; Cartesian coordinates, three lower frequencies, and single-point SCF energies for structures **IIa** and **IIb**; complete ref 16; CIF file for structures of **2a**, **2b**, **10**, **11**, and **12**; NMR spectra for compounds **2**−**12**. This material is available free of charge via the Internet at http://pubs.acs.org.

OM7006634